Title: Comparison of ultraviolet absorbance and NO-chemiluminescence for ozone measurement in wildfire plumes at the Mount Bachelor Observatory

Authors: Honglian Gao[1], Daniel A. Jaffe[1,2]

[1]University of Washington Bothell, School of Science, Technology, Engineering and Mathematics, 18115 Campus Way NE, Bothell, WA, 98011, USA

[2]University of Washington, Department of Atmospheric Sciences, 408 ATG Building, Box 351640, Seattle, WA, 98195-1640, USA

Correspondence to: Honglian Gao (hlgao@uw.edu)

Abstract

The goal of this paper is to evaluate the accuracy of the commonly used ozone (O_3) instrument (the ultraviolet (UV) photometer) against a Federal Reference Method (Nitric Oxide - chemiluminescence) for ozone measurement in wildfire smoke plumes. We carried out simultaneous ozone measurement with two UV O_3 photometers and one nitric oxide–chemiluminescence (NO-CL) ozone detectors during wildfire season (Aug. 1–Sept. 30) in 2015 at the Mount Bachelor Observatory (MBO, 2763 m above mean sea level, Oregon, USA). The UV O_3 shows good agreement and excellent correlation to NO-CL O_3, with linear regression slopes close to unity and R^2 of 0.92 for 1-h average data and R^2 of 0.93 for O_3 daily maximum 8-h average (MDA8). During this two-month period we identified 35 wildfire events. Ozone enhancements in those wildfire plumes measured by NO-CL O_3 and UV O_3 monitors also show good agreement and excellent linear correlation, with a slope and R^2 of 1.03 and 0.86 for O_3 enhancements (ΔO_3) and 1.00 and 0.98 for carbon monoxide (CO)-normalized ozone enhancement ratios ($\Delta O_3/\Delta CO$), respectively. Overall, the UV O_3 was found to have a positive bias of 4.7±2.8 ppbv compared to the NO-CL O_3. The O_3 bias between NO-CL O_3 and UV O_3 is independent of wildfire plume tracers such as CO, particulate matter (PM_1), aerosol scattering, and ultrafine particles. The results demonstrate that the UV O_3 absorbance method is reliable, even in highly concentrated wildfire plumes.

Keywords: Ozone, UV photometer, NO-chemiluminescence, wildfire

1. Introduction

Ground-level ozone (O_3) is one of the six “criteria air pollutants” identified in the Clean Air Act and regulated by the US Environmental Protection Agency (EPA) (Long et al., 2014). The EPA sets the National Ambient Air Quality Standards (NAAQS) for ozone. The O_3 NAAQS is currently 70 ppbv, which is defined as the “3-year average of the annual fourth-highest daily maximum 8-h average (MDA8) O_3 concentration” (US EPA, 2015). In the troposphere, ozone is produced from the reaction of nitrogen oxides (NO_x) and non-methane organic carbons (NMOCs) in the presence of sunlight (Finlayson-Pitts and Pitts, 2000). Ozone precursors come from natural and anthropogenic sources, such as lightning, vegetation, wildfires, and other biomass and fossil fuel combustion (Cooper et al., 2015; Sun et al., 2016). Jaffe and Widger (2012) estimated that O_3 from wildfires produces 170 Tg of O_3 per year, which contributes to 3.5% of the global tropospheric ozone budget. One recent study estimated that wildfire

smoke will impact 10-20% of the days when the MDA8 O_3 concentration exceeds the NAAQS ozone standard of 70 ppbv in most US cities and that wildfire smoke contributes 3–36 ppbv of ozone to the smoke-impacted areas (Brey and Fischer, 2015).

Because wildfires are becoming more common in the western US, Alaska, and western Canada (Dennison et al., 2014; Yang et al., 2015; Yue et. al., 2015), and due to the tightening NAAQS O_3 standard from 75 ppbv to 70 ppbv (US EPA, 2015), the issue of wildfire contributions to ozone is becoming more important. However, the O_3 production in wildfires is still poorly understood with large variations and uncertainties (Baker et al., 2016). In the review by Jaffe and Widger (2012), a large variation of -0.1 to 0.9 in O_3-to-carbon monoxide (CO) enhancement ratios were reported in wildfire plumes. To understand the wildfire contribution to ozone production, it is critical that the ozone monitoring technique be precise and accurate in wildfire plumes.

The Federal Reference Method (FRM) for measuring O_3 is gas-phase ethylene-chemilumiescence (ET-CL), based on the reaction of ozone in sampled air with an ethylene reactant gas. ET-CL ozone analyzers have been replaced by ultraviolet (UV) O_3 analyzers and the ozone Federal Equivalent Method (FEM) in the O_3 monitoring network because the UV O_3 analyzers are reliable, low cost, easy to operate, and without the need for a constant supply of a flammable and potentially explosive reactant gas (Gao et al., 2012; Long et al., 2014). These O_3 analyzers determine ozone concentration by measuring the absorption of UV light at 254 nm by the ozone molecules in the sampled air and then use the Beer-Lambert Law. Thus, any UV absorbers (absorption at 254 nm) in the light path could be potentially measured as ozone interferents by the UV O_3 detectors. Potential interferents include aromatic hydrocarbons (Leston et al., 2005; Ollison et al., 2013; Spicer et al., 2010,; Long et al., 2014), mercury (Hg) vapor (Spicer et al., 2010; US EPA, 1999), and fine particles (Dunlea et al., 2006; Payton, 2007). In wildfire plumes, there can be large amounts of particulate matter (PM), CO, and volatile organic compounds (VOCs, including aromatics and oxygenated VOCs) (Akagi et al., 2011, 2012, 2013; Yokelson et al., 2007), and these species may interfere in UV ozone monitors. The US EPA has also recently established the nitric oxide-chemiluminescence (NO-CL) O_3 method as an additional FRM for ozone measurement (US EPA, 2015). The NO-CL O_3 analyzer detects ozone based on the reaction of O_3 in sampled air with NO reactant gas forming excited nitrogen dioxide (NO_2*). The NO_2* emits a photon at 600 nm–2800 nm when it returns to its ground state. The emitted photon is then detected by a photomultiplier (PMT), and the PMT count is proportional to the O_3 numbers in the sampled air. Similar to the ET-CL analyzers, the NO-CL O_3 monitors are not significantly impacted by typical concentrations of potential ambient interferents, such as PM, hydrogen sulfide (H_2S), carbon dioxide (CO_2), nitrogen oxides (NO_x), VOCs, Hg, and sulfur dioxide (SO_2) (Long et al., 2014; US EPA, 2015). However, NO-CL and ET-CL appear to have a small interference from a water vapor (WV) change in the ambient air (Matthews et al., 1977; Lenschow et al., 1981; Ridley and Grahek, 1990; Ridley et al., 1992; Leston et al., 2005; Williams et al., 2006; Bariteau et al., 2010; Ollison et al., 2013; Boylan et al., 2014; Long et al., 2014).

Several studies have compared ozone measurements from collocated UV O_3 monitors and either ET-CL or NO-CL O_3 monitors in ambient air or in smog chambers. Kleindienst et al. (1993) found that UV O_3 monitors overestimated ozone in sampled air by 0.1 ppbv of ozone per ppbv of toluene in the air compared to an ET-CL O_3 analyzer. Ryerson et al. (1998) showed no difference by UV O_3 monitors in airborne ambient ozone measurements compared to a NO-CL O_3 monitor. Leston et al. (2005) observed a positive O_3 bias of 20–50 ppbv measured by UV O_3 analyzers equipped with manganese dioxide ($MnO_{2)}$ scrubbers compared to ET-CL O_3 monitors during humid and hot summer days. Williams et al. (2006)

found excellent agreement between UV O_3 monitors and an NO-CL O_3 analyzer in ground-based measurements at urban/industry sites and ship-borne measurements in the Gulf of Maine. Spicer et al. (2010) found a positive bias of 1 ppbv O_3 per 1 pptv of Hg vapor on UV O_3 monitors in a chamber study and a ±4.1 ppbv discrepancy between collocated conventional UV monitors and those equipped with Nafion to remove WV during the smog season. Ollison et al. (2013) showed that the bias between UV O_3 monitors and a NO-CL O_3 analyzer was greater in hot and humid August days (up to 6 ppbv) than in cooler days after mid-September. Interference in UV ozone monitors by some aromatic compounds were specifically studied in smog chambers because they absorb 254-nm UV light. The UV-MnO_2 ozone monitors overestimated ozone by 15% and 38%, respectively, in high concentrations of toluene and a mixture of C_8 aromatic hydrocarbons (o-xylene, p-xylene and ethylbenzene) (Leston, 2005). These aromatic compounds, such as toluene, benzene, stylene, and xylenes, were commonly measured in wildfire plumes (Akagi et al., 2011, 2013; Yokelson et al., 2007). This raises concerns for the accuracy of ozone measurement by UV monitors in wildfire plumes.

Payton (2007) carried out a series of laboratory experiments in a large smoke chamber to investigate the effects of wildfire smoke on UV ozone instruments with a PFA inlet filter to remove particles. Four UV O_3 monitors were collocated with a NO-CL O_3 detector and an ET-CL O_3 detector to measure ozone in a total of 19 burns of a variety of potential fire fuel mixes. $PM_{2.5}$ density was continuously monitored during these chamber experiments. Compared to the ET-CL monitor, positive O_3 biases were measured by UV O_3 monitors in a range of 1–14.6 (ppbv O_3 per 100 µg m^{-3} of $PM_{2.5}$) with means of 6.1–6.6 (ppbv O_3 per 100 µg m^{-3} of $PM_{2.5}$) in the fresh (plume age 0–6 hours) wood fire smoke. However, O_3 concentrations were generally low in these studies and no ambient comparisons were made.

How aged wildfire plumes affect UV photometric O_3 monitors is still an unanswered question. In this study, we are the first to investigate the interference on ozone measurements in aged wildfire plumes using the most commonly used UV O_3 analyzers with MnO_2 scrubbers. In order to address this issue, we set up two UV photometric ozone monitors side by side along with a custom-built NO-CL ozone analyzer, which is free of significant interference from other pollutants in ambient air (Long et al., 2014; US EPA, 2015). We made simultaneous ozone measurement at Mt. Bachelor Observatory from Aug. 1 to Sept. 30, 2015. During summer 2015, wildfire smoke was abundant in the Pacific Northwest (Laing et al., 2016), giving rise to a useful data set for this study.

2. Experimental methods

2.1 Site description and collocated instrumentation

Mount Bachelor Observatory (MBO) is a well-established mountaintop site that has been in operation since February 2004 (Gratz et al., 2015). It is one of the few mountain sites sampling lower tropospheric baseline ozone along the 1800-km US West Coast (Cooper et al., 2015, Gratz et al., 2015). MBO is located on the summit of Mount Bachelor, an isolated volcanic peak located in the Deschutes National Forest in the Cascades Mountains of central Oregon, USA. (43.979 ^{o}N, 121.687^{o}W, 2763 m above sea level). The nearest cities are 31 km (Bend, Oregon, pop. 76,639) and 53 km (Redmond, Oregon, pop. 26,215) to the east. Due to its topography and lack of local anthropogenic emissions, previous studies have shown that MBO is an ideal site to observe Asian long-range transport of pollution, Asian and regional biomass burning plumes and subsidence of O_3-rich air masses from the upper troposphere/lower stratosphere (UTLS) (Ambrose et al., 2011; Baylon et al., 2014, 2016; Briggs et al., 2016; McClure et al., 2016; McKendry et al., 2011; Reidmiller et al., 2010; Weiss-Penzias et al., 2006; Wigder et al., 2013a, 2013b).

In addition to ozone measurements, a suite of collocated chemicals (CO, CO_2, NO_x, PAN), aerosols (submicron dry aerosol scattering (σ_{sp}), the dry particle mass under 1 μm (PM1), and ultrafine particles number concentrations (UFP)), and meteorological parameters (wind speed, wind direction, pressure, temperature, relative humidity, and water vapor) were continuously measured at MBO during the summer of 2015. Aerosol scattering was measured by a multi-wavelength integrating nephelometer (model 3563, TSI Inc., Shoreview, MN) at wavelengths 450,550, and 700 nm. The σ_{sp} at 550 nm was used in this paper. The UFP was measured with a TSI 3938 scanning mobility particle sizer (SMPS), with a TSI 3082 electrostatic classifier, a TSI 3081 differential mobility analyzer (DMA) and a TSI 3787 waterbased condensation particle counter. PM_1 was measured with an optical particle counter (OPC, model 1.109, Grimm Technologies, Douglasville, GA). Methods for those observations were reported in our previous publications (Ambrose et al., 2011; Baylon et al., 2014; Fischer et al., 2010a, 2010b; Laing et al., 2016). σ_{sp} , PM_1, and UFP were corrected to standard temperature and pressure (STP at 273.15 K and 101.325 kPa)

The air sampling inlets for gaseous and aerosol measurements were located about 4 m above the highest point on the roof of the Mt. Bachelor summit ski lift building. The instruments were housed in two temperature-controlled rooms (20±2 ^oC) inside the building, approximate 15 m below the inlet. All instruments for gaseous species, including O_3, PAN, NO_x, and CO/CO_2, were connected to a common Teflon manifold. The manifold was connected to ¼" ID and 5/8" OD PFA tubing from the gaseous sample inlet on the roof with a 1 μm Teflon particle filter. The inlet filter was changed every 2 to 3 weeks or when it was dirty during the intensive summer campaign. This filter removes essentially all aerosols. Total flow through the manifold was about 20 standard liters per minute (SLPM), corresponding to a residence time of about 2 seconds in the manifold (Reidmiller et al., 2010; Fischer et al., 2010a; Ambrose et al., 2011). The aerosol measurements were made from a separate aerosol inlet (0.688" conductive tubing) and using an impactor, which is designed to sample aerosols with aerodynamic diameter less than 1 μm (Ambrose et al., 2011; Fischer et al., 2011; Laing et al., 2016; Reidmiller et al., 2010).

2.2 Ozone instruments

2.2.1 Instruments and setup

We used a custom-built, high-sensitivity NO/O_3 chemiluminescence (NO-CL) detector as a reference to investigate the potential interference from aged wildfire plumes on UV photometric ozone analyzers. Two standard UV photometric ozone analyzers with conventional MnO_2 scrubbers (Dasibi 1008-RS and Ecotech Serinus 10) were set up side by side with the NO-CL ozone analyzer. The three ozone analyzers were connected to the same Teflon manifold to sample particle-free ambient air. Figure 1 shows the schematic of the custom-built NO-CL O_3 analyzer and the two collocated UV photometric ozone analyzers.

The NO-CL O_3 instrument was previously used to measure reactive nitrogen oxides (NO_y) at MBO (Baylon et al., 2014; Briggs et al., 2016). The original design was reported by Ridley and Grahek (1990). The details of the reaction chamber and detector were described by Honrath (1991) and Beine (1996). The gold-plated reaction chamber volume is 250 cm^3. The reaction chamber temperature was controlled at 30±0.1 ^oC and the pressure was 3.2 torr. The reaction chamber was coupled to a red-sensitive (600–2800 nm) photomultiplier tube (PMT), which was efficiently cooled down with a thermoelectric refrigerated chamber (Products for Research, Model TEI 82TSRF008) to about -18 ^oC (about 38 ^oC below the room temperature). The PMT power voltage was set to negative 1.71 kilovolts.

The sample air flow for the NO-CL ozone analyzer was controlled by a Tylan stainless steel mass flow controller (MFC) at 5.00×10^2 standard cubic centimeters per minute (sccm). The residence time in the reaction chamber was 0.12 seconds. A chemically pure grade nitric oxide gas in a pressurized cylinder

(99.5 % purity, 7.6 cubic feet, pressure 700 psi, Airgas, Inc.) was used as reactant gas for the NO-O_3 chemiluminescence reaction. The NO flow was maintained at 1.00 sccm by a stainless steel MFC (Tylan). Because NO is a potent toxic gas, a 24-volt electric two-way shut-off stainless steel valve was installed inline between the NO cylinder regulator valve and the MFC for emergency shut-off via remote actuation. The gas mixture left the reaction chamber through a short (0.5 cm) stainless steel tube, entered a catch-pot and was pulled out of the system via a rotary oil vacuum pump (Edwards High Vacuum International, model E2M8). Excess NO in the reaction chamber effluent was destroyed by granular potassium permanganate ($KMnO_4$) in the catch-pot. The pump exhaust then passed through an activated charcoal cartridge before it was vented to the outdoor air downwind and far away from the common inlet.

The O_3 detection cycle included a measurement phase and a zeroing phase. The measurement phase collected count rates from sampled air plus background count rates, and the zeroing phase collected only the background count rates. Zeroing was enabled for 15 minutes every four hours. During the measurement phase, pure NO was delivered directly to mix with sampled air in the reaction chamber (red arrow in Figure 1a). During the zeroing phase, the pure NO flow was diverted to mix with sampled air in the zeroing volume (a Teflon volume of about 100 cm^3) upstream to the reaction chamber (green arrow in Figure 1a). The O_3 in the sampled air was titrated by excess pure NO in the zeroing volume, and the NO+O_3 chemiluminescence reaction happened out of view of the PMT. Thus, only the background count rate, which is the sum of dark count and photoemission from other species, was recorded by the PMT. The background count rate for each 10-second measurement point during the four-hour detection cycle was calculated by linear interpolation from the two zeroing readings before and after each measuring phase. The difference in count rates between the measurement count rate and the background count rate is the ambient O_3 count rate.

The data acquisition and system automation, including the NO emergency shut-off valve and the measurement/zeroing cycle switching solenoids, were controlled by a LabJack U12 (LabJack Corp.) and the DAQFactory software (AzeoTech, Inc.) on a PC laptop.

2.2.2 Calibration and QC

On-site zero air was generated by pulling room air through an electric air dryer (Tekran Air Dryer, model 1102) followed by an activated charcoal cartridge and a PFA filter. A known O_3 concentration for multi-point onsite calibration by transfer standard or field standard was generated using this dry zero air.

a. Ozone calibration in dry zero air

The two UV photometric ozone analyzers (Dasibi 1008-RS and Ecotech Serinus 10) were manually calibrated side by side every three months with a transfer standard certified by the Washington State Department of Ecology (WADOE Transfer Standard SN:6452). We also performed an automated weekly zero check for one hour using the zero air generated on-site. The method detection limit (MDL) for the Dasibi 1008-RS and the Ecotech Serinus 10 is 1 ppbv, with an uncertainty of ±2 % in hourly data for O_3 concentrations higher than 5 ppbv (Ambrose et al., 2011; Weiss-Penzias et al., 2006). The transfer standard was a Dasibi 1008-PC ozone generator/analyzer that was never exposed to ambient air and was certified annually by the WADOE. Another Dasibi 1008-RS ozone analyzer/generator was calibrated against the WADOE transfer standard side by side with the NO-CL ozone analyzer at MBO at the beginning of this study. The calibrated Dasibi 1008-RS served as a field standard O_3 generator for an in situ daily span check and to conduct multi-point calibrations, which were carried out both in the

beginning and at the end of this study. Zero air with ozone concentrations of 0–500 ppbv were generated by the field standard O_3 generator and sampled simultaneously by both the UV and NO-CL O_3 analyzers for calibration. The reduced major axis (RMA) regression analysis between the ozone field standard and the transfer standard yielded a slope, intercept, and R^2 of 0.992, 2.5 ppbv, and 0.999, respectively, which is within the transfer standard recertification guideline (regression slope=1.00±0.01 and intercept <3 ppbv) (US EPA, 2015). The O_3 sensitivity for the custom-built NO-CL ozone analyzer was 2742 cps $ppbv^{-1}$ when NO flow was 1.50 sccm and 2030 cps $ppbv^{-1}$ at NO flow of 1.00 sccm. Taking into account both the O_3 sensitivity and the pure NO toxicity, we set the NO flow to 1.00 sccm for the NO-CL ozone measurement. A daily span check was programmed for 20 minutes at 7:00 local standard time (LST). The field standard O_3 generator was stabilized for 30 minutes prior to each daily span check. The averaged daily span check O_3 concentration was 97.8±3.0 ppbv during the two months. The average O_3 NO-CL sensitivity for the daily span check was 1995±51 cps $ppbv^{-1}$, with a precision of 2.6 % (N=50, 1σ). Both the UV and NO-CL ozone analyzers were calibrated at six known ozone levels (0–500 ppbv) on-site at the end of this fieldwork. The O_3 sensitivity for the final multi-point calibration was 2030 cps $ppbv^{-1}$ (R^2=0.999). This agrees very well with the daily span check sensitivity within the margin of uncertainty. The MDL for the NO-CL ozone analyzer was 12 pptv (3σ).

b. Ozone calibration in ambient air

Since ambient air should not be used to feed the ozone generator of either the transfer standard or the field standard, we used an ozone standard addition method to generate various ozone concentrations in ambient air to examine the effect of WV on the NO-CL O_3 and UV O_3 calibration at the end of this study. Figure 1b shows the schematic of the ambient ozone standard addition system. Ozone was generated from oxygen photolysis ($\lambda \leq 242$ nm) using a low pressure mercury lamp (Pen-Ray, 90-012-01). Then the generated ozone was diluted by an ambient air flow and delivered to the UV ozone analyzers, ozone field standard (measurement only mode), and the NO-CL O_3 analyzer for "wet" calibration. Ambient air flow with an ozone level in the range of 0–330 ppbv was obtained by controlling the amount of UV lamp irradiation exposure by covering a portion of the mercury lamp with aluminum foil. The results showed that calibrations for the UV O_3 were not affected by ambient air but were affected for NO-CL O_3. The ozone sensitivity of the NO-CL O_3 analyzer in ambient air was 1809±112 (n=5, 1σ) cps $ppbv^{-1}$, which is about 9.3% lower than that in dry zero air. This result is consistent with previous observations of negative interference from WV on NO-CL O_3 analyzers due to the WV quenching effect on the excited NO_2* (Ridley and Grahek, 1990; Ridley et al.,1992; Leston et al., 2005; Williams et al., 2006; Bariteau et al., 2010; Spicer et al., 2010; Ollison et al., 2013; Boylan et al., 2014). We used this ambient ozone sensitivity to determine NO-CL O_3 concentrations from the reference subtracted O_3 count rates.

2.3 Wildfire plume identification

Wildfire plumes were identified using a combination of observed submicron dry aerosol scattering (σ_{sp}) and CO, satellite imagery and trajectory models, similar to Baylon et al. (2014) and Widger et al. (2013b). Specifically, we used the following criteria:

1. CO concentration and aerosol scattering at 550 nm (σ_{sp}) were elevated above background, with CO ≥ 150 ppbv and $\sigma_{sp} \geq 20$ Mm^{-1} for at least one hour, and there was a strong correlation between CO and σ_{sp}, with linear regression $R^2 \geq 0.80$, using 5-min average data. The reduced major axis (RMA) regression was used in all the linear regression analyses in this paper. RMA

linear regression parameters were calculated using software for Reduced Major Axis regression for Java developed by Andrew J. Bohonak and Kim van der Linde (2004).

2. A wildfire was identified based on MODIS fire data as reported in the AirNow-Tech Navigator (https://www.airnowtech.org/navigator/index.cfm). The navigator tool allowed us to analyze air quality monitoring data, the Hazard Mapping System (HMS) smoke map, and HMS fire locations. We then used MODIS Terra and Aqua reflectance true color satellite images to confirm the fire and smoke observations.
3. To confirm the plume source, we used the Hybrid Single Particle Lagrangian Integrated Trajectory (Hysplit) model (http://ready.arl.noaa.gov/HYSPLIT.php), the 1^{o} resolution Global Data Assimilation System (GDAS) meteorological data to calculate 10-day backward trajectories (for long-range transport), and the 40 km resolution US Eta Data Assimilation System (EDAS) meteorological data to calculate 5-day backward trajectories (for regional fires) initiated from MBO. Plume age was estimated from the Hysplit trajectories based on the fire location and travel time.

3. Results and discussion

We measured O_3 with both NO-CL and UV analyzers from Aug. 1–Sept. 30, 2015. During this period, we identified 35 wildfire events based on the criteria given above. This was a significant wildfire season in the Pacific Northwest due to exceptionally warm temperatures and low snowpack during the preceding spring (Jaffe and Zhang, 2017; Mote et al., 2016). For each plume, we calculated O_3, WV, CO, and CO_2 enhancement ratios using the multiple background subtraction method proposed by Briggs et al. (2016). Basically, the average of three background values is used as background for a fire plume: the ambient concentration prior to the plume arrival, the monthly median at 16:00 LST, and the hourly concentration at 16:00 LST previous to the time the plume was observed. In practice, this method was important only to calculate the enhancement ratio of $\Delta O_3/\Delta CO$, due to the relatively high O_3 background related to the ambient O_3. Table 1 shows those results. As reported previously, the $\Delta O_3/\Delta CO$ enhancement ratios of wildfire plumes span a wide range of values; some of the plumes contain a significant amount of O_3 while others did not (Jaffe and Wigder, 2012; Baylon et al., 2014; Wigder et al., 2013b). At present, we have a very limited understanding of what causes these variations (Jaffe and Wigder, 2012; Baylon et al., 2014).

3.1 Water vapor interference on NO-CL O_3 FRM

The two UV O_3 analyzers generated nearly identical results (with R^2 and slope of 0.99 and 1.02, respectively) so these were averaged to generate a single time series of UV O_3 (O_{3_UV}) 5-minute, 1-hour, and daily maximum 8-hour average (MDA8) data. We compared this averaged O_{3_UV} data with the NO-CL O_3 data ($O_{3\_NO\text{-}CL}$). The ozone bias (O_{3_bias}) was calculated by subtracting the $O_{3\_NO\text{-}CL}$ values from the O_{3_UV} values ($O_{3\_bias} = O_{3\_UV} - O_{3\_NO\text{-}CL}$).

For the NO-CL O_3 analyzer equipped with the inlet PFA particle filter, the only known interference for ozone measurement in the ambient air is water vapor (Spicer et al., 2010; US EPA, 2015), which quenches NO_2^* signals (Matthews et al., 1977; Ridley et al., 1992; Bariteau et al., 2010; Boylan et al., 2014). The quenching effect of WV results in a negative interference on the O_3 measurement. Laboratory studies show that relative loss of the O_3 signal from WV quenching is linearly related to the amount of WV in the sample air (Matthews et al., 1977; Ridley et al., 1992; Boylan et al., 2014). Eq. 1 has been used to calculate a WV correction for ambient ozone concentrations calculated from dry

calibration (Matthews et al., 1977; Lenschow et al., 1981; Ridley et al., 1992; Williams et al., 2006; Bariteau et al., 2010; Boylan et al., 2014).

$$O_{3\_corr} = O_{3\_mea} \times (1 + \alpha\gamma) \quad (1)$$

where O_{3_corr} is the WV-corrected O_3 mole fraction, O_{3_mea} is the value measured by the NO-CL analyzer, α is the dimensionless correction factor, and γ is the WV–to–dry air mole fraction (in mmol mol^{-1} or ‰). Lenschow et al. (1981) reported an α value of (5±1) $\times 10^{-3}$; Ridley et al. (1992) measured an α value of (4.3±0.3) $\times 10^{-3}$; and Boylan et al. (2014) determined a value of (4.15±0.14) $\times 10^{-3}$ for their fast response O_3 chemiluminescence instrument (FRCI) system.

Because the O_3 sensitivity was measured at only one WV level in ambient air, we used the ambient and dry air calibrations to estimate a dimensionless correction factor (α) for the NO-CL O_3 analyzer. During the ambient air calibration, the WV was 7.77±0.35 (mmol mol^{-1}). The difference in ozone sensitivity in dry zero air and in ambient air was 9.32%. Assuming that the WV effect on our custom-built NO-CL O_3 analyzer follows Eq. (1), and the decrease in ozone sensitivity in the ambient air was due only to WV quenching, we calculated an α value of 0.0132^3. This value is about 3 times the α value from Boylan et al. (2014) and Ridley et al. (1992). This difference might be due to instrument configurations, reaction chamber design and volume and the sample-to-reactant gas flow ratio (Matthews et al., 1977). Our custom-built NO-CL analyzer reaction chamber volume is 250 cm^{-3}, which is about 6 times that of Boylan et al. (2014) and 15 times that of Ridley et al. (1992). We also note that our study was not intended to measure the α, so this test was done only once.

We applied α values of 0.0132 and 0.0045 to correct the WV quenching effect on 5-min and 1-h NO-CL O_3 data, respectively. Figure 2 shows scatter plots of the ozone bias ($O_{3\_bias} = O_{3\_UV} - O_{3\_NO\text{-}CL}$) against WV for uncorrected (α=0) and corrected NO-CL O_3 data (α=0.0045 and α=0.0132). Figure 2a shows a slightly positive trend in ozone bias calculated from uncorrected (α=0) $O_{3\_NO\text{-}CL}$ as WV increases, with a mean ozone bias of 4.14±2.86 ppbv. If we use an α value of 4.5×10^{-3} from the literature, similar to Ridley et al. (1992) and Boylan et al. (2014), as in Figure 2b, there is no dependence between the O_3 bias and WV, with a mean ozone bias of 4.74±2.84 ppbv. Figure 2c is the scatter plot of the ozone bias against WV with $O_{3\_NO\text{-}CL}$ corrected by an extrapolated α of 0.0132. The ozone bias shows a slightly negative trend as the WV increases, with a mean of 5.56±3.18 ppbv. Comparing Figures 2a–c, we see that when the α value increases from 0 to 0.0045 to 0.0132, the dependence of ozone bias (O_{3_bias}) on WV changes from a positive trend, to an almost flat line, then to a negative trend, respectively. This result shows that the NO-CL O_3 analyzer is affected by WV and our measured α value of 0.0132 may be too large. We further analyzed the correlation between O_{3_UV} and the WV corrected $O_{3\_NO\text{-}CL}$ with α=0, α=0.0045 and α=0 .0132 respectively and looked at ozone enhancements in wildfire plumes. We found that the value of α does not affect the linear correlation between O_{3_UV} and $O_{3\_NO\text{-}CL}$ in ambient air nor the correlations between ozone enhancements in wildfire plumes (ΔO_{3_UV} and $\Delta O_{3\_NO\text{-}CL}$). Also, correcting the $O_{3\_NO\text{-}CL}$ data using different values of α does not affect the dependence of ozone bias on the wildfire plume tracers (such as CO, PM_1, σ_{sp}, and ultrafine particles). We presented the results for α=0.0045 in this paper. The results for $O_{3\_NO\text{-}CL}$ corrected using α=0 and α=0.0132 are included in Figures S1–S7 in the Supplemental Information.

The linear regression analysis for $O_{3\_NO\text{-}CL}$ and O_{3_UV} yields a slope, an intercept and an R^2 of 1.00±0.01, (-4.73)±0.39 ppbv and 0.920, respectively. In the 1-h average data, the WV correction increases ozone values in the range of 0.1 to 8.6 ppbv, with a mean of 3.5 ppbv and a median of 3.5 ppbv. In the latest NAAQS for the O_3 FRM for both the ET-CL and NO-CL O_3 analyzers (US EPA, 2015), an

air dryer is required to remove WV from sampled air upstream to the ozone analyzers to minimize the WV interference in ozone monitoring. A Nafion membrane was used in a few studies to remove WV and mitigate the WV effect on ET-CL or NO-CL O_3 measurements (Bariteau et al., 2010; Spicer et al., 2010; Boylan et al., 2014).

3.2 Comparison of UV O_3 and NO-CL O_3 data

The 1-h time series for the UV O_3 (O_{3_UV}) and NO-CL O_3 ($O_{3\_NO\text{-}CL}$) are plotted in Figure 3. The UV O_3 and NO-CL O_3 measurements follow each other very well, showing the same trends and structures in ozone profile and generally excellent agreement with each other.

The scatter plot in Figure 4a shows a strong correlation between hourly O_{3_UV} and $O_{3\_NO\text{-}CL}$ data with an R^2 of 0.920, a slope of 1.00±0.01, and an intercept of -4.73±0.39 ppbv. During our two-month measurement period, $O_{3\_NO\text{-}CL}$ is in the range of 19.0–78.0 ppbv, with a mean of 45.6 ppbv, and a median of 44.9 ppbv; O_{3_UV} is in the range of 24.2–82.6 ppbv, with a mean and a median of 50.4 and 50.1, respectively. The UV O_3 averaged slightly higher with a 4.7 ppbv offset. Similarly, Ryerson et al. (1998) found that the UV absorption instrument measured slightly higher ozone than the NO-CL O_3 analyzer in the airborne study of ozone in power plant plumes. The discrepancy was traced to a decrease in the photon counting efficiency in flight. In response, Ryerson et al. (1998) multiplied the NO-CL O_3 data by the in-flight average O_{3_UV}–to–$O_{3\_NO\text{-}CL}$ ratio of 1.045. A relatively large bias between NO-CL O_3 and UV O_3 was observed during Aug. 11–14. During this period we see no evidence for instrument malfunction in either NO-CL O_3 or UV O_3 analyzers. The bias could not be explained by either humidity or measured pollutants. While we have no good explanation for the bias during this period, including these data in our analysis does not affect the results and conclusions.

Considering that NAAQS O_3 compliance is based on the maximum daily 8-h average (MDA8) of ozone, we calculated the MDA8 for both NO-CL O_3 and UV O_3. Figure 4b shows the strong correlation between the NO-CL O_3 MDA8 and the UV O_3 MDA8, with a slope of 1.04±0.04, R^2 of 0.93 and intercept of -7.07±2.05 ppbv. As with the hourly averages, the MDA8 measured by UV O_3 shows slightly higher values compared to the NO-CL O_3, but overall excellent agreement.

3.3 Mt. Bachelor Observatory wildfire plumes

To investigate the effect of aerosol and gaseous pollutants on the UV photometric ozone measurement, we plotted the 1-h average ozone bias against wildfire plume indicators (e.g., CO, PM_1, ultrafine particles) and dry aerosol scattering at 550 nm (σ_{sp}). The scatter plots of CO, σ_{sp}, PM_1, and ultrafine particles (UFP) are shown in Figures 5a, 5b, 5c, and 5d, respectively. All of these plots show a similar pattern: no positive or negative relationship between ozone bias and CO, σ_{sp}, PM_1, and UFP. The elevated σ_{sp}, UFP, and CO values indicate pollution events, mostly from wildfires smoke as seen at MBO during summer. This result indicates that, with the inlet filter in place, as is required for O_3 FEM and O_3 FRM (US EPA, 2015), the wildfire gaseous pollutants do not significantly affect UV photometric ozone measurements. In addition, the ozone bias between O_{3_UV} and $O_{3\_NO\text{-}CL}$ was not affected by high ambient aerosols or gaseous pollutants concentrations during this study.

The 5-min average MBO dataset was used for wildfire event identification, enhancements, and enhancement ratio calculation. According to the plume identification criteria in Section 2.3, we identified 35 wildfire events during Aug.1 – Sept. 30, 2015. Table 1 summarizes the characteristics of these identified plumes, including plume start/end time, origin, age, and ozone enhancement ratios (RMA regression slope to CO). Because we were looking at the smoke interference on UV ozone photometer,

some bigger plumes were divided into smaller events according to the correlation between aerosol scattering σ_{sp} and CO, which focuses more on chemical variance rather than the source of the plumes. Among these 35 wildfire events, 28 events were smoke from regional wildfires in the northwest of the US, including northern California (CA), Oregon (OR), and Washington (WA); 7 events (events 16–22) were wildfire smoke heavily influenced by Siberian forest wildfires via Asian long-range transport (ALRT) (Laing et al., 2016).

The normalized submicron dry aerosols mass enhancement ratios ($\Delta PM_1/\Delta CO$) for the identified plumes were in the range of 0.18 – 0.45 µg m^{-3} $ppbv^{-1}$, with a mean of 0.29±0.07 µg m^{-3} $ppbv^{-1}$, similar to previous observation of 0.06 – 0.42 µg m^{-3} $ppbv^{-1}$ in 32 wildfire plumes at MBO reported by Wigder et al. (2013b). The CO-normalized ozone emission ratios, $\Delta O_{3\_UV}/\Delta CO$ values were in the range of (-0.031)–0.408 ppbv $ppbv^{-1}$, with a mean of 0.070±0.084 (1σ) ppbv $ppbv^{-1}$, and $\Delta O_{3\_NO\text{-}CL}/\Delta CO$ values were in the range of (-0.021) – 0.303, with a mean of 0.070±0.078 (1σ) ppbv $ppbv^{-1}$. Both sets of ratios are within the $\Delta O_3/\Delta CO$ ratio of (-0.1)–0.9 ppbv $ppbv^{-1}$ in wildfire plumes reviewed by Jaffe and Wigder (2012). The ratios are also close to the $\Delta O_3/\Delta CO$ ratio of 0.01– 0.51 ppbv $ppbv^{-1}$ for wildfire plumes observed at MBO by Wigder et al. (2013b). The modified combustion efficiency (MCE, calculation method details in Biggs, et al. (2016)) for the plumes is 0.87– 0.99, with a mean of 0.95±0.03. The plume ages are estimated to range from 6 hours to 6–7 days for ALRT from Siberian forest fires. The ΔPM_1 and ΔCO are linearly correlated for all the identified plumes, with an overall slope of 0.28 µg m^{-3} $ppbv^{-1}$. The $\Delta PM_1/\Delta CO$ enhancement ratio for the individual wildfire plumes is 0.19–0.58 µg m^{-3} $ppbv^{-1}$, which is typical for wildfires (Wigder et al., 2013b).

3.4 UV photometric O_3 analyzer performance in the wildfire plumes

For each wildfire plume we calculated an O_3 enhancement (ΔO_3), normalized O_3 enhancement ratio ($\Delta O_3/\Delta CO$) by ratio of enhancements ($\Delta O_3$and ΔCO) method and linear regression (between O_3 and CO) method, using both UV O_3 and NO-CL O_3. Linear regression analysis in Figure 6a shows a strong correlation between ozone enhancement measured in plumes by the UV O_3 (ΔO_{3_UV}) analyzer and the NO-CL O_3 ($\Delta O_{3\_NO\text{-}CL}$) analyzer, with a slope of 1.03±0.07, an intercept of -0.20±0.90 ppbv, and an R^2 of 0.86. Not all wildfire plumes show an O_3 enhancement, so not all plumes have a CO and O_3 correlation. Figure 6b presents the correlation between the O_{3_UV}-to-CO and $O_{3\_NO\text{-}CL}$-to-CO RMA regression slopes for 9 wildfire plumes in which both O_{3_UV} and $O_{3\_NO\text{-}CL}$ are linearly correlated to CO with $R^2 \geq 0.60$. This excellent correlation between O_{3_UV}-to-CO and $O_{3\_NO\text{-}CL}$-to-CO enhancement ratios yields a slope of 1.00±0.04, an intercept of (-4.96 ± 2.28) $\times 10^{-3}$ ppbv $ppbv^{-1}$ and an R^2 of 0.983. The strong correlations between O_{3_UV} and NO-CL $O_{3\_NO\text{-}CL}$ enhancement in wildfire plumes (Figures 6a and 6b) demonstrate that the UV O_3 monitors were not affected by the wildfire plumes. The ozone enhancement bias (ΔO_{3_bias} = ΔO_{3_UV} - $\Delta O_{3\_NO\text{-}CL}$) in the individual wildfire plumes are plotted against the enhancement of wildfire plume indicators (ΔCO, $\Delta\sigma_{sp}$, ΔUFP, and ΔPM_1) in Figure S8 for α=0, in Figure S9 for α=0.0045, and in Figure S10 for α=0.0132 in $O_{3\_NO\text{-}CL}$ correction. All the RMA regression results are listed in Table S1. The independence between ΔO_3 bias and the gaseous and aerosol wildfire plume indicators (ΔCO, $\Delta\sigma_{sp}$, ΔUFP, and ΔPM_1) further confirms that the UV O_3 photometer is not affected by wildfire plumes, regardless of the α value used in NO-CL O_3 correction.

A previous chamber study showed that UV O_3 monitors were positively biased by fresh biomass burning (BB) smoke. Payton (2007) measured ozone in BB smoke from a large combustion chamber simultaneously with four UV O_3 monitors, one ET-CL O_3 detector, and one NO-CL O_3 analyzer from a common inlet with a Teflon filter. He reported a strong linear correlation between ozone bias (UV O_3

435 minus ET-CL O_3) and the $PM_{2.5}$ level in fresh BB smoke from 19 burns, with 1 to 14.6 ppbv O_3
436 interference on UV O_3 per 100 µg m^{-3} of $PM_{2.5}$ and a mean of 5.1–6.6 ppbv O_3 per 100µg m^{-3} $PM_{2.5}$ in the
437 BB smoke (Payton, 2007). However, this study examined O_3 concentrations in an indoor facility with no
438 new ozone formation. Thus it is difficult to interpret these results with respect to ambient air quality
439 monitors. Our results indicate no bias in UV O_3 monitors at PM levels up to 288 µg m^{-3} and CO levels up
440 to 1076 ppbv.
441 We estimated potential interference on UV O_3 measurement by aromatic VOC in wildfire plumes.
442 Because there is no direct measurement for aromatic species, we estimated the concentrations of aromatic
443 compounds based on the literature according to the emission factors of CO and aromatic VOCs (e.g.,
444 benzene, toluene, ethylbenzene, (p,m,o)-xylene, propylbenzene, ethyltoluene, and trimethylbenzene) in
445 BB plumes (Akagi et al., 2012; Yokelson et al., 2007), using CO as a tracer. We estimated that a related
446 emission factor for aromatic VOCs in BB plumes is 3.43 (ppbv per ppmv of CO). An aromatic VOCs
447 interference study by Leston et al. (2005) showed that UV O_3 analyzers overestimated O_3 by 0.28% with
448 1 ppbv of aromatic VOCs in the sampled air. Using these two factors, we estimated that on average the
449 aromatic compounds co-emitted with 1 ppm of CO in the wildfire plumes will give the UV O_3 monitor a
450 positive bias of 1% O_3 response. The CO enhancement in the 35 identified wildfire plumes ranged from
451 44–909 ppbv (with a mean of 277±208 ppbv) and the average NO-CL O_3 is 49.0 ppbv in this study.
452 Therefore, the aromatic compounds in the plumes could cause 0.02–0.42 ppbv (mean of 0.13±0.10 ppbv)
453 O_3 interference on the UV O_3 monitors. This number is much smaller than the UV O_3 instrument
454 precision of 2% at 50 ppbv O_3.
455 We also estimated potential interference on UV O_3 by mercury in wildfire plumes. Spicer et al.
456 (2010) reported 1 ppbv of O_3 interference from 1 pptv of mercury in sampled air. Finley et al. (2009)
457 observed a total atmospheric mercury (TAM) emission rate from biomass plumes of 1.4±0.6 pg m^{-3} per
458 ppbv of CO. If 1 ppm of CO is seen in a wildfire plume, then TAM concentration in the plume is about
459 1.4±0.6 ng m^{-3}, or 0.2 pptv, which could cause O_3 interference of 0.2 ppbv, again a value that is
460 significantly smaller than the UV O_3 instrument uncertainty of 2%.
461
462 **4. Conclusions**
463 We compared the two ozone measurement techniques at MBO during the 2015 wildfire season.
464 The results from UV O_3 and NO-CL O_3 monitors are well correlated. The 1-h average UV O_3 and NO-CL
465 O_3 RMA linear regression analysis results in a slope, an intercept, and an R^2 of 1.00±0.01, -4.7±0.4 ppbv
466 and 0.92, respectively. The RMA linear regression analysis for MDA8 O_{3_UV} and MDA8 $O_{3\_NO\text{-}CL}$ yields a
467 slope, an intercept, and an R^2 of 1.04±0.04, -7.1±2.0 ppbv, and 0.93, respectively. The UV method is
468 biased higher by approximately 4.7±2.8 ppbv.
469 We observed a total of 35 wildfire events during the two-month observation period with PM_1 and
470 CO enhancements up to134 µg m^{-3} and 909 ppbv, respectively. We found an excellent correlation
471 between the ozone enhancements and CO-normalized ozone enhancement ratios of the UV O_3 and the
472 NO-CL O_3. The small ozone bias between the UV O_3 and the NO-CL O_3 was not correlated to any
473 wildfire plume tracers (CO, σ_{sp}, UFP, PM_1). The excellent correlation between the two ozone
474 measurements and lack of dependence between ozone bias and wildfire plume indicators shows that the
475 ozone FEM measurement by UV photometers is reliable even in highly concentrated wildfire plumes.
476 The NO-CL O_3 analyzer showed some interference from water vapor in air due to the WV
477 quenching on excited NO_2^*. Based on one calibration, we found a quenching effect factor of 0.0132,
478 which is about three times higher than the previously reported results. However, correcting the NO-CL O_3

data with three quenching factors of 0, 0.0045 and 0.0132 changed the UV O_3 and NO-CL O_3 bias slightly but had no impact on our overall conclusions.

5. References

Akagi, S. K., Craven, J. S., Taylor, J. W., McMeeking, G. R., Yokelson, R. J., Burling, I. R., Urbanski, S. P., Wold, C. E., Seinfeld, J. H., Coe, H., Alvarado, M. J. and Weise, D. R. (2012) Evolution of trace gases and particles emitted by a chaparral fire in California. Atmospheric Chemistry and Physics, 12, 1397-1421.

Akagi, S. K., Yokelson, R. J., Burling, I. R., Meinardi, S., Simpson, I., Blake, D. R., McMeeking, G. R., Sullivan, A., Lee, T., Kreidenweis, S., Urbanski, S., Reardon, J., Griffith, D. W. T., Johnson, T. J. and Weise, D. R. (2013) Measurements of reactive trace gases and variable O3 formation rates in some South Carolina biomass burning plumes. Atmospheric Chemistry and Physics, 13, 1141-1165.

Akagi, S. K., Yokelson, R. J., Wiedinmyer, C., Alvarado, M. J., Reid, J. S., Karl, T., Crounse, J. D. and Wennberg, P. O. (2011) Emission factors for open and domestic biomass burning for use in atmospheric models. Atmospheric Chemistry and Physics, 11, 4039-4072.

Ambrose, J. L., Reidmiller, D. R. and Jaffe, D. A. (2011) Causes of high O(3) in the lower free troposphere over the Pacific Northwest as observed at the Mt. Bachelor Observatory. Atmospheric Environment, 45, 5302-5315.

Baker, K. R., Woody, M. C., Tonnesen, G. S., Hutzell, W., Pye, H. O. T., Beaver, M. R., Pouliot, G. and Pierce, T. (2016) Contribution of regional-scale fire events to ozone and PM2.5 air quality estimated by photochemical modeling approaches. Atmospheric Environment, 140, 539-554.

Bariteau, L., Helmig, D., Fairall, C. W., Hare, J. E., Hueber, J. and Lang, E. K. (2010) Determination of oceanic ozone deposition by ship-borne eddy covariance flux measurements. Atmos. Meas. Tech., 3, 441-455.

Baylon, P., Jaffe, D. A., Wigder, N. L., Gao, H. and Hee, J. (2014) Ozone enhancement in western US wildfire plumes at the Mt. Bachelor Observatory: The role of NOx. Atmospheric Environment, 109, 297-304.

Baylon, P. M., Jaffe, D. A., Pierce, R. B. and Gustin, M. S. (2016) Interannual Variability in Baseline Ozone and Its Relationship to Surface Ozone in the Western US. Environmental Science & Technology, 50, 2994-3001.

Beine, H. J. (1996) NOx Photochemistry in High Northern Latitudes during spring (A Ph.D. dissertation).

Bohonak, A. J. and Linde, K. v. d. (2004) RMA: Software for Reduced Major Axis regression, Java version. Website: http://www.kimvdlinde.com/professional/rma.html.

Boylan, P., Helmig, D. and Park, J. H. (2014) Characterization and mitigation of water vapor effects in the measurement of ozone by chemiluminescence with nitric oxide. Atmos. Meas. Tech., 7, 1231-1244.

Briggs, N. L., Jaffe, D. A., Gao, H., Hee, J. R., Baylon, P. M., Zhang, Q., Zhou, S., Collier, S. C., Sampson, P. D. and Cary, R. A. (2016) Particulate Matter, Ozone, and Nitrogen Species in Aged Wildfire Plumes Observed at the Mount Bachelor Observatory. Aerosol and Air Quality Research, 16, 3075-3087.

Brey, S. J. and Fischer, E. V. (2015) Smoke in the City: How Often and Where Does Smoke Impact Summertime Ozone in the United States? Environmental Science & Technology, 50, 1288-1294.

Cooper, O. R., Langford, A. O., Parrish, D. D. and Fahey, D. W. (2015) Challenges of a lowered U.S. ozone standard. Science, 348, 1096-1097.

Gao, R. S., Ballard, J., Watts, L. A., Thornberry, T. D., Ciciora, S. J., McLaughlin, R. J. and Fahey, D. W. (2012) A compact, fast UV photometer for measurement of ozone from research aircraft. Atmos. Meas. Tech., 5, 2201-2210.

Dennison, P. E., Brewer, S. C., Arnold, J. D. and Moritz, M. A. C. G. L. (2014) Large wildfire trends in the western United States, 1984–2011. Geophysical Research Letters, 41, 2928-2933.

Dunlea, E. J., Herndon, S. C., Nelson, D. D., Volkamer, R. M., Lamb, B. K., Allwine, E. J., Grutter, M., Ramos Villegas, C. R., Marquez, C., Blanco, S., Cardenas, B., Kolb, C. E., Molina, L. T. and Molina, M. J. (2006) Technical note: Evaluation of standard ultraviolet absorption ozone monitors in a polluted urban environment. Atmos. Chem. Phys., 6, 3163-3180.

Finlayson-Pitts, B. and Pitts, J. N., Jr. (2000) Chemistry of the Upper and Lower Atmosphere: Theory, Experiments, and Applications, Academic Press, San Diego, Calif.

Finley, B. D., Swartzendruber, P. C. and Jaffe, D. A. (2009) Particulate mercury emissions in regional wildfire plumes observed at the Mount Bachelor Observatory. Atmospheric Environment, 43, 6074-6083.

Fischer, E. V., Jaffe, D. A., Marley, N. A., Gaffney, J. S. and Marchany-Rivera, A. (2010a) Optical properties of aged Asian aerosols observed over the US Pacific Northwest. Journal of Geophysical Research-Atmospheres, 115.

Fischer, E. V., Jaffe, D. A., Reidmiller, D. R. and Jaeglé, L. (2010b) Meteorological controls on observed peroxyacetyl nitrate at Mount Bachelor during the spring of 2008. Journal of Geophysical Research, 115, D03302.

Fischer, E. V., Jaffe, D. A. and Weatherhead, E. C. (2011) Free tropospheric peroxyacetyl nitrate (PAN) and ozone at Mount Bachelor: potential causes of variability and timescale for trend detection. Atmospheric Chemistry and Physics, 11, 5641-5654.

Gratz, L. E., Jaffe, D. A. and Hee, J. R. (2015) Causes of increasing ozone and decreasing carbon monoxide in springtime at the Mt. Bachelor Observatory from 2004 to 2013. Atmospheric Environment, 109, 323-330.

Honrath, R. E. (1991) Nitrogen Oxides in the Artic Troposphere. (Ph.D. dissertation).

Jaffe, D. A. and Wigder, N. L. (2012) Ozone production from wildfires: A critical review. Atmospheric Environment, 51, 1-10.

Jaffe, D. A. and Zhang, L. (2017) Meteorological anomalies lead to elevated O_3 in the western U.S. in June 2015. Geophysical Research Letters, DOI: 10.1002/2016GL072010

Kleindienst, T. E., Hudgens, E. E., Smith, D. F., McElroy, F. F. and Bufalini, J. J. (1993) Comparison of Chemiluminescence and Ultraviolet Ozone Monitor Responses in the Presence of Humidity and Photochemical Pollutants. Air & Waste, 43, 213-222.

Laing, J. R., Jaffe, D. A. and Hee, J. R. (2016) Physical and Optical Properties of Aged Biomass Burning Aerosol from Wildfires in Siberia and the Western US at the Mt. Bachelor Observatory. Atmos. Chem. Phys. Discuss., 2016, 1-27.

Lenschow, D. H., Pearson, R. and Stankov, B. B. (1981) Estimating the ozone budget in the boundary layer by use of aircraft measurements of ozone eddy flux and mean concentration. Journal of Geophysical Research: Oceans, 86, 7291-7297.

Leston, A. R., Ollison, W. M., Spicer, C. W. and Satola, J. (2005) Potential Interference Bias in Ozone Standard Compliance Monitoring. Journal of the Air & Waste Management Association, 55, 1464-1472.

566 Long, R., Hall, E., Beaver, M., Duvall, R., Kaushik, S., Kronmiller, K., Wheeler, M., Garvey, S., Drake,
567 Z. and McElroy, F. (2014) Performance of the Proposed New Federal Reference Methods for
568 Measuring Ozone Concentrations in Ambient Air. U.S. Environmental Protection Agency,
569 Washington, DC, EPA/600/R-14/432 (NTIS PB2015-101240), 2014.
570 Matthews, R. D., Sawyer, R. F. and Schefer, R. W. (1977) Interferences in chemiluminescent
571 measurement of nitric oxide and nitrogen dioxide emissions from combustion systems.
572 Environmental Science & Technology, 11, 1092-1096.
573 McClure, C. D., Jaffe, D. A. and Gao, H. L. (2016) Carbon Dioxide in the Free Troposphere and
574 Boundary Layer at the Mt. Bachelor Observatory. Aerosol and Air Quality Research, 16, 717-728.
575 McKendry, I., Strawbridge, K., Karumudi, M. L., O'Neill, N., Macdonald, A. M., Leaitch, R., Jaffe, D.,
576 Cottle, P., Sharma, S., Sheridan, P. and Ogren, J. (2011) Californian forest fire plumes over
577 Southwestern British Columbia: lidar, sunphotometry, and mountaintop chemistry observations.
578 Atmospheric Chemistry and Physics, 11, 465-477.
579 Mote, P. W., Rupp, D. E., Li, S., Sharp, D. J., Otto, F., Uhe, P. F., Xiao, M., Lettenmaier, D. P., Cullen,
580 H. and Allen, M. R. C. G. L. (2016) Perspectives on the causes of exceptionally low 2015
581 snowpack in the western United States. Geophysical Research Letters, 43, 10,980-988.
582 Ollison, W. M., Crow, W., and Spicer, C. W. (2013) Field testing of new-technology ambient air ozone
583 monitors. Journal of the Air & Waste Management Association, 63, 855-863.
584 Payton, R. (2007) Final Report for the "Effects of Wildfire Smoke on UV Ozone Instruments" Regional
585 Applied Research Effort. Air Technical Assistance Unit US EPA Region 8, 1-69.
586 Reidmiller, D. R., Jaffe, D. A., Fischer, E. V., and Finley, B. (2010) Nitrogen oxides in the boundary
587 layer and free troposphere at the Mt. Bachelor Observatory. Atmospheric Chemistry and Physics,
588 10, 6043-6062.
589 Ridley, B. A. and Grahek, F. E. (1990) A Small, Low Flow, High Sensitivity Reaction Vessel for NO
590 Chemiluminescence Detectors. Journal of Atmospheric and Oceanic Technology, 7, 307-311.
591 Ridley, B. A., Grahek, F. E. and Walega, J. G. (1992) A Small High-Sensitivity, Medium-Response
592 Ozone Detector Suitable for Measurements from Light Aircraft. Journal of Atmospheric and
593 Oceanic Technology, 9, 142-148.
594 Ryerson, T. B., Buhr, M. P., Frost, G. J., Goldan, P. D., Holloway, J. S., Hübler, G., Jobson, B. T.,
595 Kuster, W. C., McKeen, S. A., Parrish, D. D., Roberts, J. M., Sueper, D. T., Trainer, M., Williams,
596 J. and Fehsenfeld, F. C. (1998) Emissions lifetimes and ozone formation in power plant plumes.
597 Journal of Geophysical Research: Atmospheres, 103, 22569-22583.
598 Spicer, C. W., Joseph, D. W. and Ollison, W. M. (2010) A Re-Examination of Ambient Air Ozone
599 Monitor Interferences. Journal of the Air & Waste Management Association, 60, 1353-1364.
600 Sun, L., Xue, L., Wang, T., Gao, J., Ding, A., Cooper, O. R., Lin, M., Xu, P., Wang, Z., Wang, X., Wen,
601 L., Zhu, Y., Chen, T., Yang, L., Wang, Y., Chen, J. and Wang, W. (2016) Significant increase of
602 summertime ozone at Mount Tai in Central Eastern China. Atmos. Chem. Phys., 16, 10637-10650.
603 US EPA (1999) Laboratory Study to Explore Potential Interferences to Air Quality Monitors. EPA-
604 454/C-00-002, Office of Air Quality Planning and Standards.
605 US EPA (2015) National Ambient Air Quality Standards for Ozone; Final Rule, 80 FR 65291 (October
606 26, 2015).
607 Weiss-Penzias, P., Jaffe, D. A., Swartzendruber, P., Dennison, J. B., Chand, D., Hafner, W. and Prestbo,
608 E. (2006) Observations of Asian air pollution in the free troposphere at Mount Bachelor
609 Observatory during the spring of 2004. Journal of Geophysical Research-Atmospheres, 111.

Wigder, N. L., Jaffe, D. A., Herron-Thorpe, F. L. and Vaughan, J. K. (2013a) Influence of daily variations in baseline ozone on urban air quality in the United States Pacific Northwest. Journal of Geophysical Research-Atmospheres, 118, 3343-3354.

Wigder, N. L., Jaffe, D. A., and Saketa, F. A. (2013b) Ozone and particulate matter enhancements from regional wildfires observed at Mount Bachelor during 2004-2011. Atmospheric Environment, 75, 24-31.

Williams, E. J., Fehsenfeld, F. C., Jobson, B. T., Kuster, W. C., Goldan, P. D., Stutz, J. and McClenny, W. A. (2006) Comparison of Ultraviolet Absorbance, Chemiluminescence, and DOAS Instruments for Ambient Ozone Monitoring. Environmental Science & Technology, 40, 5755-5762.

Yang, J., Tian, H., Tao, B., Ren, W., Pan, S., Liu, Y. and Wang, Y. C. J. G. (2015) A growing importance of large fires in conterminous United States during 1984–2012. Journal of Geophysical Research: Biogeosciences, 120, 2625-2640.

Yokelson, R. J., Karl, T., Artaxo, P., Blake, D. R., Christian, T. J., Griffith, D. W. T., Guenther, A. and Hao, W. M. (2007) The Tropical Forest and Fire Emissions Experiment: overview and airborne fire emission factor measurements. Atmospheric Chemistry and Physics, 7, 5175-5196.

Yue, X., Mickley, L. J., Logan, J. A., Hudman, R. C., Martin, M. V. and Yantosca, R. M. (2015) Impact of 2050 climate change on North American wildfire: consequences for ozone air quality. Atmospheric Chemistry and Physics, 15, 10033-10055.

6. Acknowledgements

The Mount Bachelor Observatory is supported by the National Science Foundation (grant #AGS-1447832) and the National Oceanic and Atmospheric Administration (contract #RA-133R-16-SE-0758).

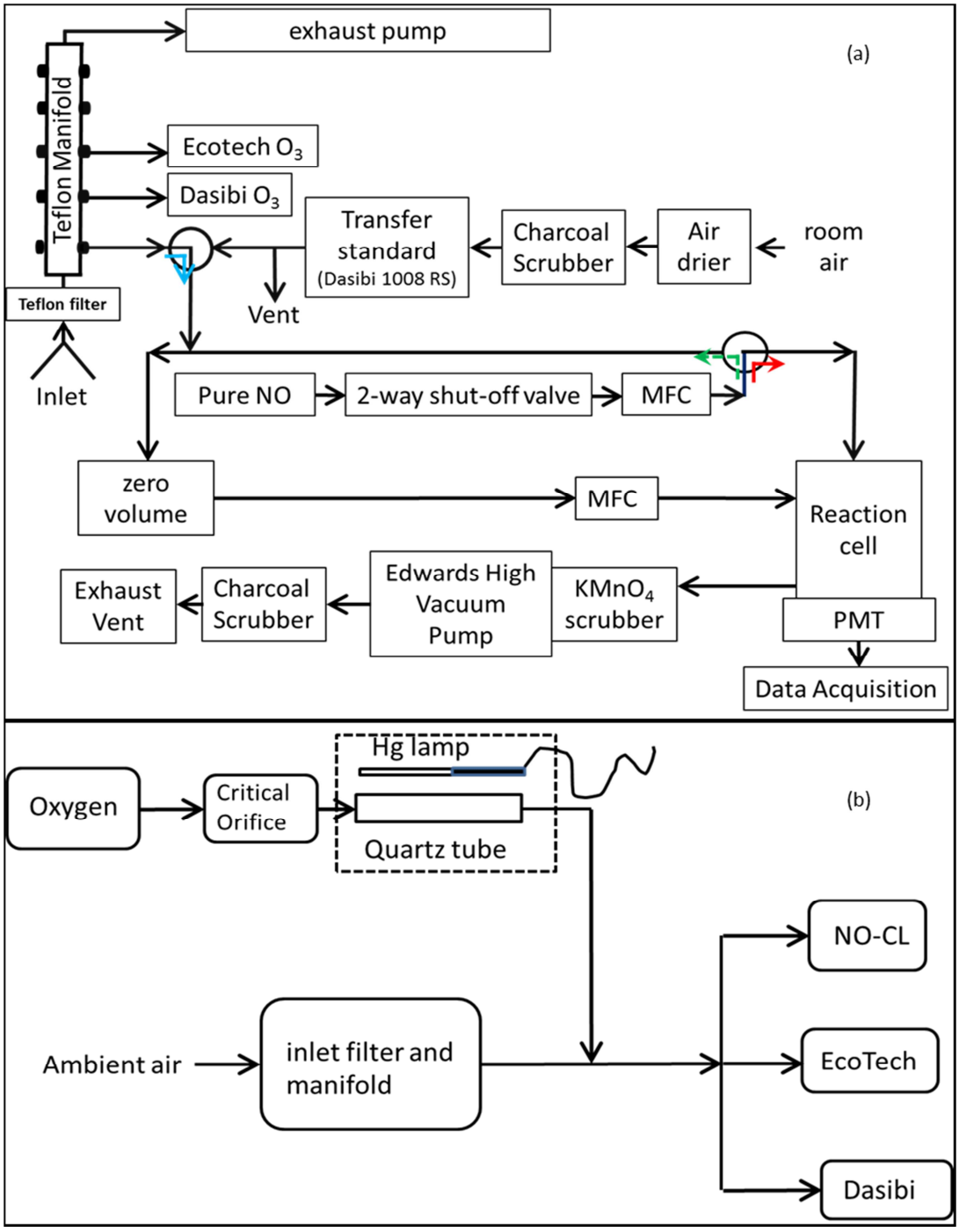

Figure 1. (a) A schematic flow chart of the custom-made NO-chemiluminescence ozone analyzer and the collocated UV ozone photometers. (b) A schematic flow chart of the ozone generation system for standard ozone addition to the ambient air for the O_3 sensitivity test by the NO-CL O_3 analyzer in ambient conditions. The blue arrow shows the flow when the sampling/calibration solenoid is in sampling mode; the green and red arrows show the flow path when the NO solenoid is in the zeroing phase or measuring phase, respectively.

645

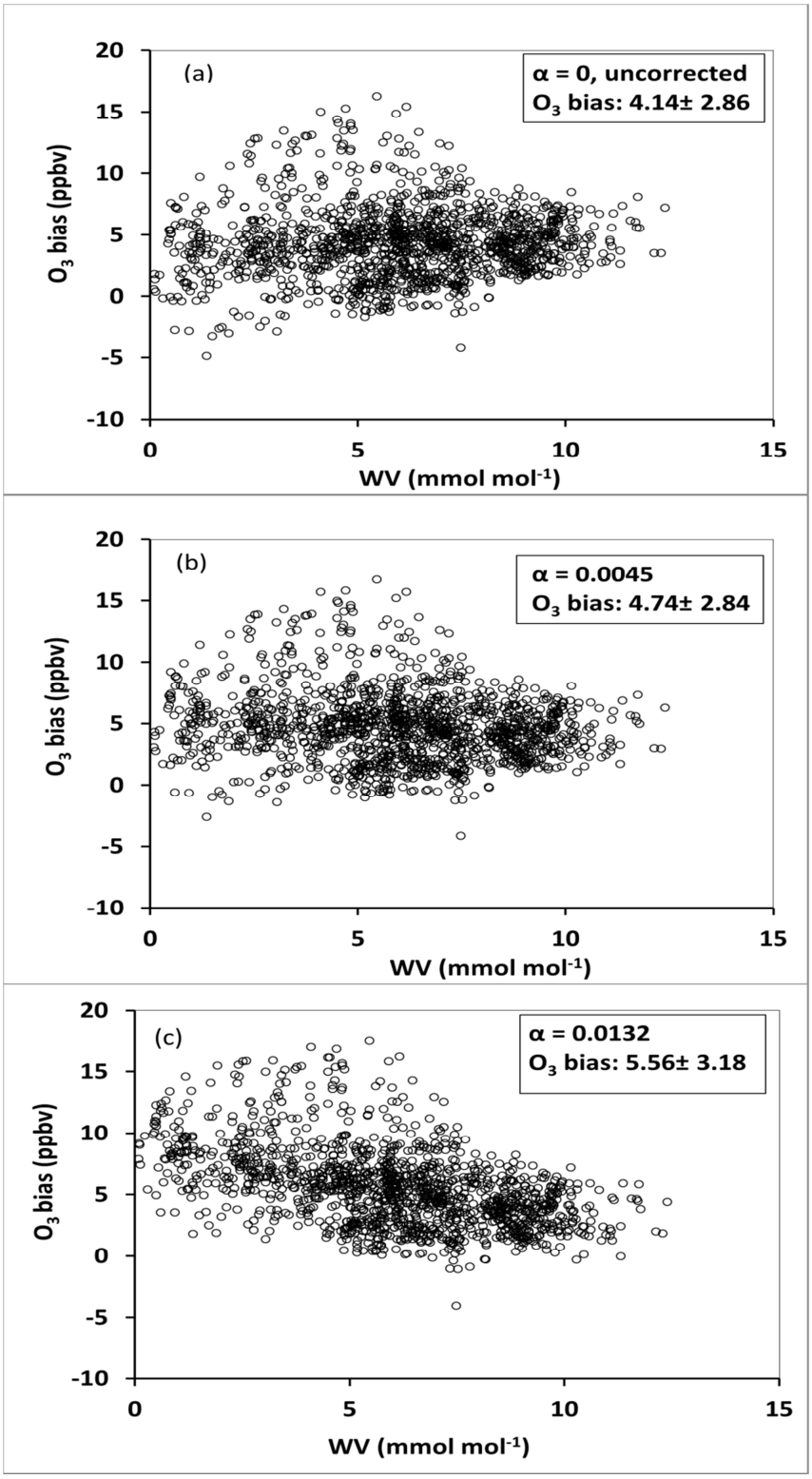

646

647 Figure 2. Scatter plots of ozone bias against ambient water vapor (WV) using 1-h average data with
648 various WV quenching effect correction factors for NO-CL O_3: (a) α=0; (b) α=0.0045; (c) α=0.0132.

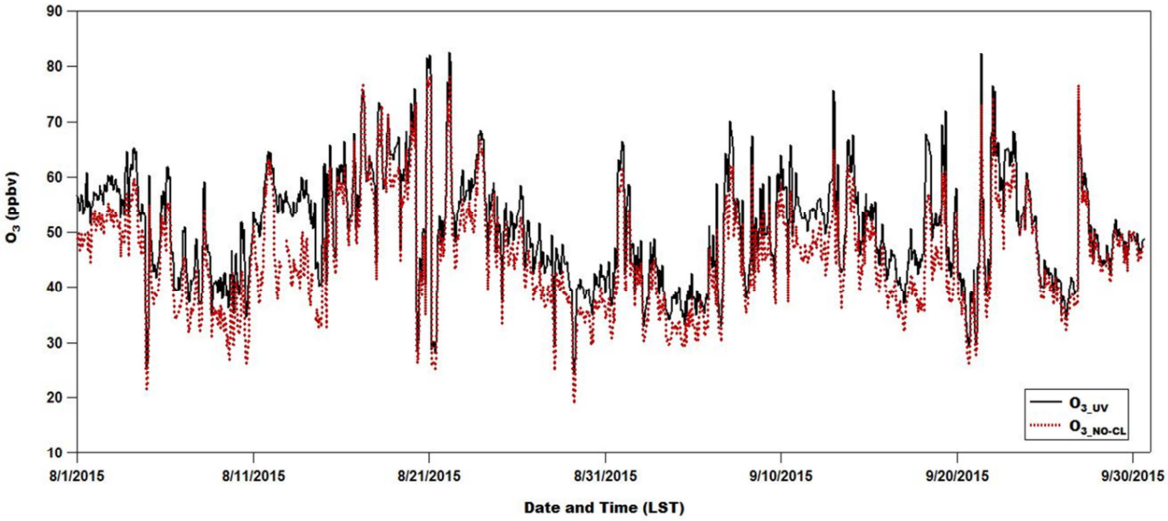

Figure 3. Time series of 1-h average O_3 mole ratio measured by the NO-CL ($O_{3\_NO\text{-}CL}$) and UV photometric (O_{3_UV}) ozone analyzers from Aug. 1 to Sept. 30, 2015, at Mt. Bachelor Observatory. The

NO-CL O_3 data have been corrected with α=0.0045.

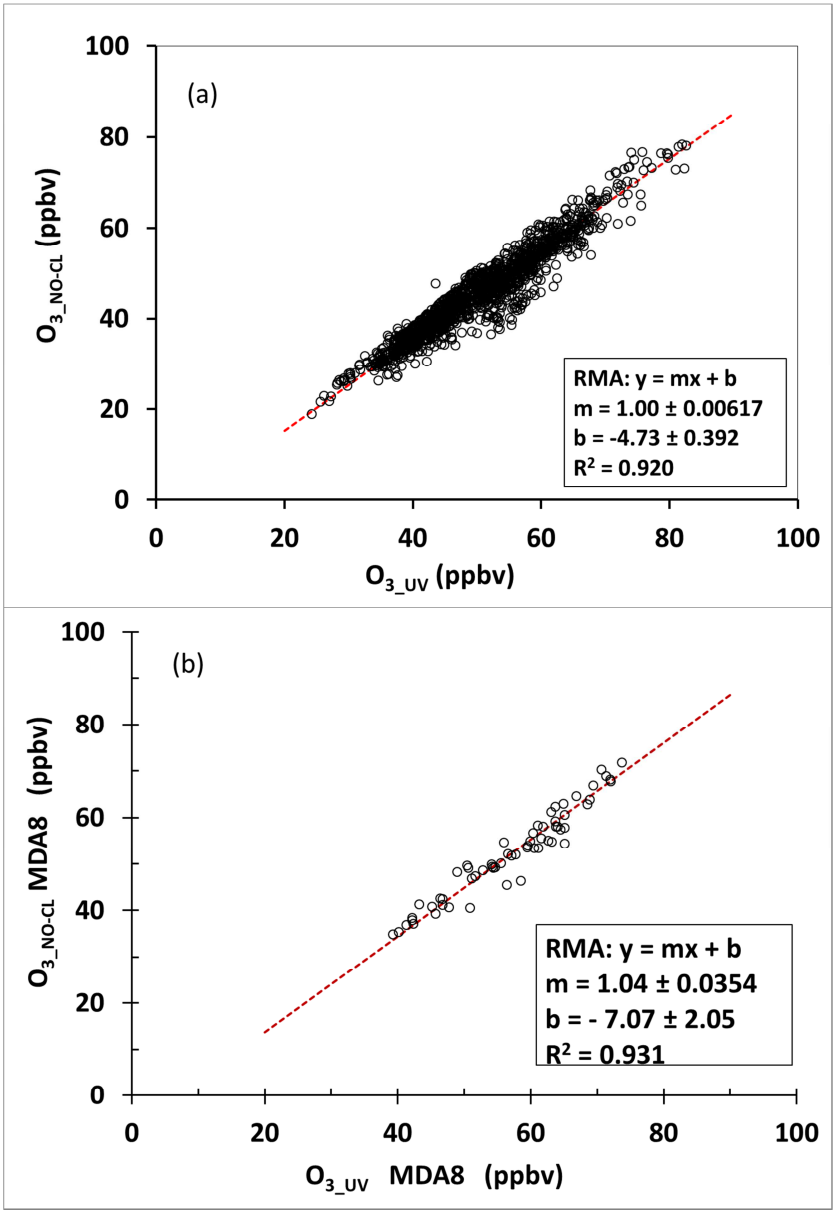

Figure 4. Correlation between ozone measured by the UV O_3 photometers (O_{3_UV}) and the NO-chemiluminescence ($O_{3\_NO\text{-}CL}$) ozone analyzers at Mt. Bachelor Observatory from Aug. 1 to Sept. 30, 2015. (a) All 1-hour average ozone data and (b) MDA8 ozone data, observed. RMA linear regression was calculated using software for Reduced Major Axis regression for Java developed by Andrew J. Bohonak and Kim van der Linde (2004). The NO-CL O_3 data have been corrected for water vapor interference with α=0.0045.

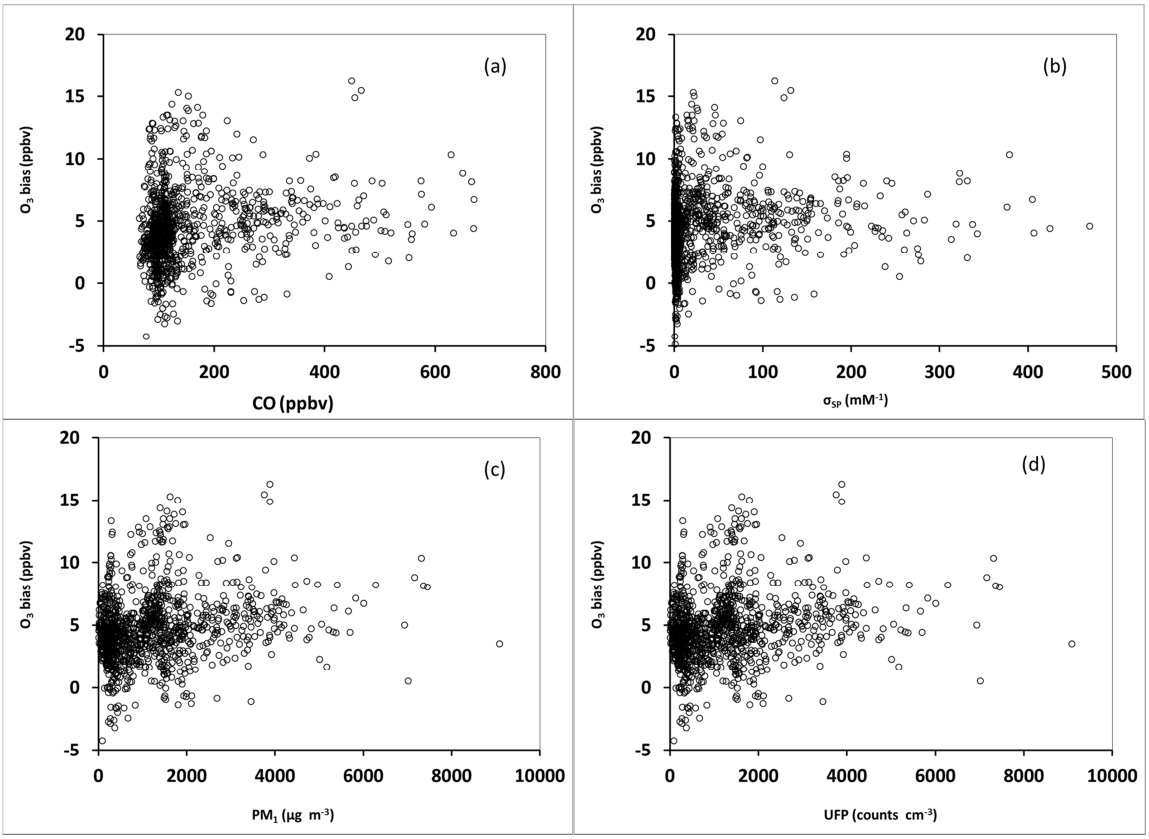

Figure 5. Scatter plots of hourly ozone bias ($O_{3\_NO\text{-}CL\_wv}$-O_{3_UV}) against wildfire event indicators measured at Mt. Bachelor Observatory from Aug. 1 to Sept. 30, 2015. Wildfire plume indicators include (a) CO, (b) aerosol scattering (σ_{sp}) at 550 nm, (c) PM_1 and (d) ultrafine particles (UFP). $O_{3\_NO\text{-}CL}$ was corrected for water vapor quenching effect with α=0.0045. Corresponding plots with α=0 and α=0.0132 are included in the Supplemental Material.

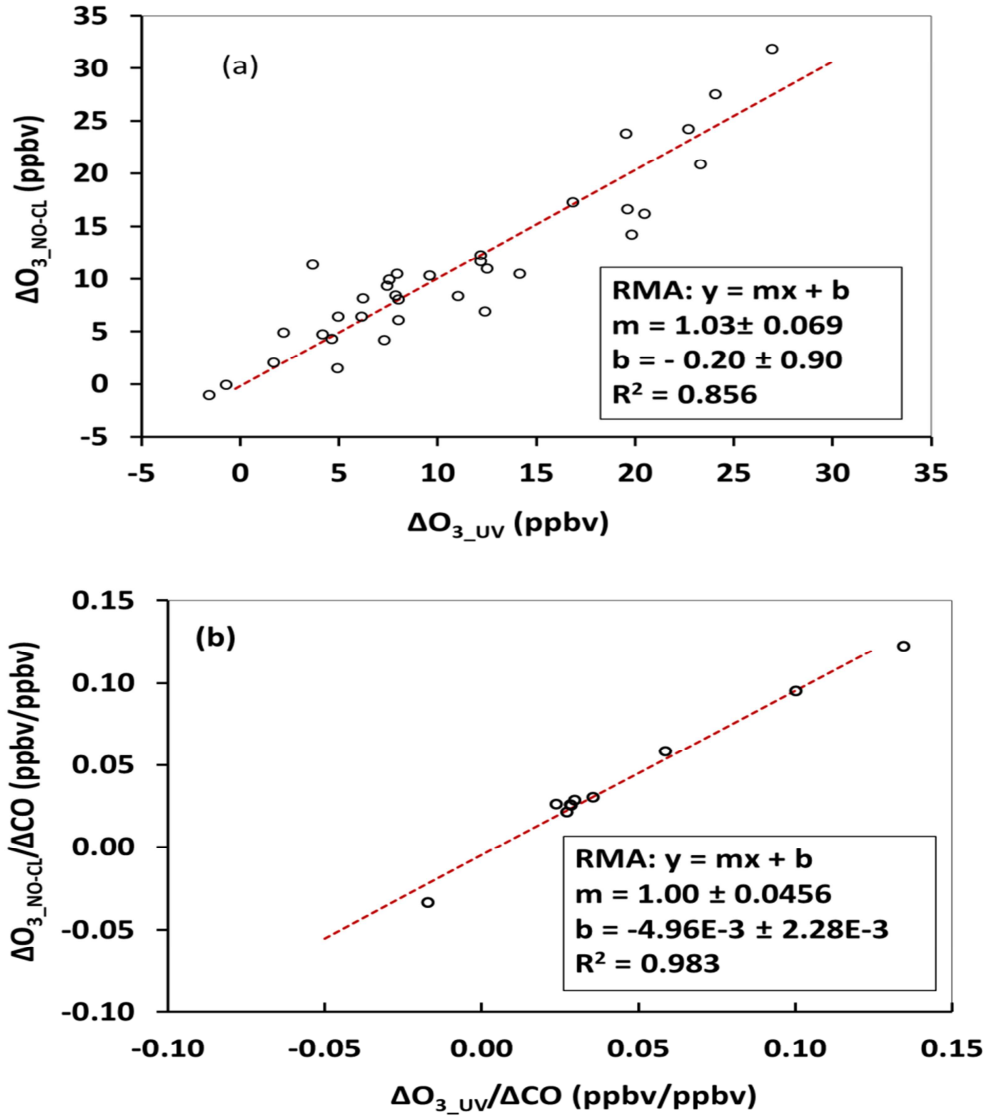

Figure 6. Linear correlation analysis between O_3 enhancements in the wildfire plumes measured by the NO-CL ($\Delta O_{3\_NO\text{-}CL}$) and UV O_3 photometers (ΔO_3_UV) from Aug. 1 to Sept. 30, 2015, at Mt. Bachelor Observatory. (a) Ozone enhancement ratios for all 35 wildfire events (n=34); (b) CO-normalized ozone enhancement ratios for 9 wildfire events in which O_3 and CO were well correlated with $R^2 \geq 0.6$ (n=9).

679 Table 1. The 35 wildfire events identified at Mt. Bachelor Observatory during Aug. 1, 2015–Sept. 30,
680 2015
681

Wildfire Events #	Start Time (UTC)	End Time (UTC)	Source	Plume Age	MCE	σ_{sp}/CO (Mm^{-1}/ppbv)	PM_1/CO ($\mu g\ m^{-3}$/ppbv)	$O_{3\_NO\text{-}CL}$ / CO (ppbv/ppbv)	O_{3_UV} / CO (ppbv/ppbv)	ΔCO (ppbv)	ΔO_{3_UV} (ppbv)	$\Delta O_{3\_NO\text{-}CL}$ (ppbv)
1	8/9/15 2:10	8/9/15 8:35	OR	12-18h	0.96±0.08	0.562	0.284	0.026	0.027	172.0	1.68	2.15
2	8/9/15 16:50	8/9/15 20:00	CA/OR	18-40h	0.94±0.09	0.789	0.368	0.021	0.022	286.0	4.89	1.55
3	8/10/15 3:20	8/10/15 6:00	CA/OR	6-18h	0.91±0.03	0.669	0.272	0.026	0.027	909.2	12.14	12.75
4	8/10/15 6:45	8/10/15 10:25	CA/OR	6-12h	0.95±0.04	0.707	0.322	0.029	0.030	378.2	7.85	8.72
5	8/10/15 11:40	8/10/15 14:35	CA	12-18h	0.97±0.05	0.598	0.290	WC	WC	185.5	-0.75	-0.05
6	8/10/15 14:25	8/10/15 19:15	CA/OR	24-32 h	0.92±0.07	0.743	0.286	0.025	0.026	668.7	14.12	10.90
7	8/10/15 19:30	8/10/15 20:45	CA	24-30h	0.96±0.07	0.465	0.197	WC	WC	193.5	6.12	6.69
8	8/10/15 20:50	8/10/15 23:05	CA	48h	0.98±0.04	0.894	0.462	0.123	0.127	170.4	12.36	7.16
9	8/11/15 0:15	8/11/15 7:50	OR	48-54h	0.98±0.07	0.498	0.302	WC	WC	124.1	3.64	11.79
10	8/13/15 23:30	8/14/15 1:45	OR	<10h	0.99±0.11	0.295	0.235	WC	WC	58.9	7.29	4.37
11	8/14/15 2:05	8/14/15 7:40	OR	12-18h	0.99±0.12	0.382	0.294	WC	WC	41.3	7.43	9.72
12	8/14/15 9:10	8/14/15 15:50	OR/CA	24-30h	0.92±0.08	0.317	0.185	-0.034	-0.035	387.1	7.92	10.89
13	8/14/15 17:30	8/14/15 22:00	OR/CA	24-30h	0.98±0.05	0.821	0.582	WC	WC	83.7	12.41	NA
14	8/14/15 22:45	8/15/15 0:40	CA	24-48h	0.94±0.26	1.205	NA	WC	WC	50.6	-1.58	-1.07
15	8/15/15 6:10	8/15/15 11:55	OR/CA	30-42h	0.99±0.08	0.509	0.294	WC	WC	48.6	19.82	14.73
16	8/16/15 23:05	8/17/15 5:20	Siberia	6-7d	0.94±0.06	0.861	NA	0.058	0.060	330.2	22.69	25.05
17	8/17/15 15:40	8/18/15 7:40	Siberia	6-7d	0.98±0.06	0.685	NA	WC	WC	118.9	26.92	32.95
18	8/18/15 14:00	8/19/15 8:40	Siberia	6-7d	0.97±0.02	0.969	NA	WC	WC	197.0	24.04	28.50
19	8/19/15 10:30	8/19/15 17:00	Siberia	6-7d	0.92±0.11	0.792	NA	WC	WC	256.7	19.58	17.23
20	8/19/15 17:45	8/20/15 2:00	Siberia	6-7d	0.97±0.08	0.782	NA	WC	WC	140.0	20.47	16.76
21	8/22/15 15:00	8/22/15 21:10	Siberia	6-7d	0.94±0.05	1.276	0.420	WC	WC	465.7	23.28	21.58
22	8/22/15 22:20	8/23/15 8:00	Siberia	6-7d	0.98±0.08	0.718	0.368	0.095	0.099	95.1	12.17	12.09
23	8/23/15 15:40	8/24/15 7:40	CA/OR	6-54h	0.98±0.01	0.694	0.235	WC	WC	477.1	19.53	24.60
24	8/24/15 7:30	8/24/15 12:20	CA/OR	12-24h	0.90±0.12	0.794	0.253	WC	WC	490.5	16.83	17.89
25	8/24/15 16:35	8/24/15 21:30	CA/OR	6-24h	0.93±0.09	0.970	0.350	WC	WC	507.9	9.58	10.70
26	8/25/15	8/25/15	CA/OR	18-42h	0.87±0.14	0.659	0.277	0.030	0.031	372.7	7.99	8.37

	4:35	7:00										
27	8/25/15 9:20	8/25/15 15:00	CA/OR	18-32h	0.91±0.11	0.612	0.288	WC	WC	354.6	7.52	10.33
28	8/25/15 15:30	8/26/15 19:05	CA/OR	18-24h	0.91±0.08	0.531	0.213	WC	WC	348.7	4.63	4.51
29	8/26/15 14:15	8/27/15 2:20	OR	6-12h	0.95±0.04	0.484	0.236	WC	WC	285.0	11.00	8.69
30	8/27/15 2:20	8/27/15 23:30	CA/OR	<6h	0.90±0.07	0.556	0.229	WC	WC	656.9	7.98	6.31
31	8/28/15 19:00	8/29/15 6:45	OR/CA	12-18h	0.95±0.06	0.435	0.236	WC	WC	277.7	4.15	4.92
32	9/10/15 11:55	9/10/15 15:45	CA/OR	24-32h	0.98±0.14	0.492	0.331	WC	WC	67.7	12.47	11.40
33	9/12/15 9:00	9/12/15 15:25	OR	6h	0.98±0.15	0.699	0.398	WC	WC	62.3	6.21	8.45
34	9/12/15 16:00	9/12/15 20:05	OR	12-18h	0.97±0.12	0.393	0.216	WC	WC	105.9	4.93	6.68
35	9/12/15 20:15	9/12/15 22:40	OR	12-18h	0.99±0.07	0.355	NA	WC	WC	91.6	2.18	5.08
Mean					0.95±0.08	0.663	0.301	0.040	0.041	270.3	10.84	11.25

Note: NA = data not available; WC = weak correlation**, (**R^2<0.6).

Highlights

1. UV is consistent with NO-CL in mountaintop O_3 measurement.

2. UV agrees with NO-CL in O_3 enhancement during 35 wildfire events.

3. The UV O_3 photometer is reliable in aged wildfire plumes.